


Reliability-based performance design optimization for seismic retrofit of reinforced concrete buildings with fiber-reinforced polymer composites

Advances in Structural Engineering
1–14
© The Author(s) 2017
Reprints and permissions:
sagepub.co.uk/journalsPermissions.nav
DOI: 10.1177/1369433217733760
journals.sagepub.com/home/ase


Xiaokang Zou¹, Qian Wang² and Jiurong Wu³

Abstract

Fiber-reinforced polymer composites can be externally bonded to reinforced concrete members which provide an effective seismic retrofit strategy for reinforced concrete structures. For seismic retrofit of a complex building structure, due to the large number of structural members, an optimum design which ensures the use of the minimum amount of fiber-reinforced polymer to achieve a given level of seismic performance is highly desirable for economic reasons. In addition, such an optimum design approach is best built on a probabilistic basis so that various sources of uncertainties in the design process can be appropriately accounted for. This work therefore studies an efficient reliability-based optimization approach for the seismic retrofit design of reinforced concrete structures using fiber-reinforced polymer composites. The structural performance is assessed at the system level using nonlinear pushover analyses. In the proposed approach, the inelastic interstorey drift ratios are modeled as indeterministic variables to consider the uncertainties of earthquake loading. By contrast, the thickness of the fiber-reinforced polymer jacket is considered as a deterministic design variable. The reliability-based design approach is formulated by minimizing fiber-reinforced polymer cost subject to prescribed structural reliability constraints. Using the results of nonlinear static pushover analyses and reliability analyses, the reliability index constraints are explicitly formulated with respect to the deterministic design variables based on the virtual work principle as well as Taylor series expansion. A numerical optimality criteria method is derived and programmed to solve this reliability-based nonlinear retrofit design optimization problem. A design example is included to illustrate the application of the new optimization approach.

Keywords

earthquakes, fiber-reinforced polymers, performance design, pushover analysis, reinforced concrete, reliability, retrofit, structural optimization

Introduction

It is well-known that many uncertainties are involved in structural designs, especially in the case of seismic resistant designs (Beck et al., 1998; Charney, 2000; Frangopol, 1985; Gaxiola-Camacho et al., 2017; Lagaros et al., 2008; Zou et al., 2010). The structural responses under random excitations such as seismic loads cannot be precisely predicted; therefore, such design problems involve considerable uncertainties (Ghobarah et al., 2000). Although the probabilistic approach has been widely adopted in the design codes of most countries, its application in building structures is limited to structural member design using partial safety factors. That is, current design codes primarily focus on the ultimate safety check of structural members including beams and columns. A structural design based on current code procedures may not guarantee a satisfactory level of system reliability. Indeed, a system

behavior has been regarded more important than a member behavior because of the high redundancy in building structures (Cheng et al., 1998; Kim and Wen, 1990).

Performance-based seismic design, which can directly address the inelastic deformation induced in

¹China State Construction Engineering (Hong Kong) Limited, Hong Kong, China

²Department of Civil & Environmental Engineering, Manhattan College, Riverdale, NY, USA

³Guangzhou University and Tamkang University Joint Research Center for Engineering Structure Disaster Prevention and Control, Guangzhou University, Guangzhou, China

Corresponding author:

Xiaokang Zou, China State Construction Engineering (Hong Kong) Limited, 29/F China Overseas Building, 139 Hennessy Road, Hong Kong, China.

Email: cezxc@yahoo.com; connie_zou@cohl.com

buildings by earthquakes, has become a standard for seismic design (Applied Technology Council (ATC), 1996; Chan and Zou, 2004; Fragiadakis et al., 2006; Gaxiola-Camacho et al., 2017; Lagaros et al., 2008; Zameeruddin and Sangle, 2016; Zou et al., 2007a). The pushover analysis method has been widely used in the performance-based design procedure to assess the nonlinear seismic performance of structures (Zou and Chan, 2005; Zou, 2012). Moreover, the performance design procedure should be based on probabilistic approaches, which account for the various sources of uncertainties and approximations as stated in FEMA-445 (FEMA, 2006). A system reliability-based design approach should be employed directly, instead of using the member level partial factor approach as adopted in the design codes currently available. Furthermore, since the peak seismic interstory drift over the lifetime of a structure is uncertain, a performance parameter can be used and directly related to the reliability index of interstory drift (Beck et al., 1998).

Although the deterministic structural design optimization has been widely used (Chan and Zou, 2004; Zou, 2012; Zou et al., 2014), the deterministic optimal structures may usually have higher failure probabilities (Frangopol and Klisinski, 1989). Structural reliability analysis methods shall be integrated into the reliability-based structural optimization process, in order to optimize structures with uncertainties. In the past few decades, reliability-based structural optimization has gained much research attention. Reliability-based optimization has special advantages over deterministic design optimization by considering reliability constraints. It provides a good balance among the structural reliability, initial cost, and other objectives, where specified performance requirements are satisfied.

Moses (1969) provided an early survey on reliability-based optimal design, and it was presented that the use of overall structural failure probability together with reliability-based design should produce more balanced designs and develop rational structural safety. Several formulations of reliability-based design optimization problems were proposed in the literatures (Frangopol, 1997). Foley (2002) reviewed the state-of-the-art and presented the vision of seismic performance-based design optimization. Performance-based optimization includes deterministic, semi-deterministic, and reliability-based (fully probabilistic) optimization. There is a need to develop reliability-based performance design optimization for structures under seismic loads (Bertero and Bertero, 2002; Charney, 2000). The randomness in the structural responses due to the uncertainties in the seismic loads can be very influential and must be considered (Ang and Cornell, 1974; Beck et al., 1998; Bertero and Bertero, 2002; Wen, 1995). In addition, extensive research has been

performed on reliability-based optimization and applications to the design of structural systems (Chang et al., 1994; Cheng et al., 1998; Frangopol and Moses, 1994; Kim and Wen, 1990; Li, 2003). In these works, related reliability constraints are inexplicitly expressed with respect to the design variables in reliability-based optimization.

The seismic interstory drift ratio of reinforced concrete (RC) frames and its probability distribution were studied by Li and Cheng (2002). Various types of uncertainties were considered, including those from the seismic loads, dead loads, live loads, structural member dimensions, and material elastic module. It was concluded that the seismic interstory drift ratios and the earthquake action have the same type of probability distribution, that is, extreme value type II. In the work of Li (2003), it was found that in steel frames, the probability distribution of the maximum elastoplastic drift ratio is related to its mean value. Earthquake loads and distribution are the dominant factors that affect the uncertainties of structural responses, when the mean drift is not large. This was also observed by other researchers (Song and Ellingwood, 1999; Wen, 2001).

Fiber-reinforced polymer (FRP) composites have been widely accepted in the retrofit of RC structures due to the fact that they can provide effective confinement to RC members to increase their strength and ductility (Cao and Ronagh, 2014; Teng et al., 2003; Teng and Lam, 2004; Shin et al., 2016; Yu et al., 2015; Yuan and Wu, 2017). Retrofit design optimization methods of RC structures using FRP jackets have been studied in recent years (Choi, 2017; Choi et al., 2014; Zou et al., 2007b). Zou et al. (2007b), developed a computer-based deterministic optimization approach for drift performance retrofit design of FRP-confined RC structures subject to seismic performance criteria. However, there is still a lack of research about reliability-based retrofit design optimization of FRP-confined RC structures. It is necessary to integrate retrofit design optimization with reliability analyses for nonlinear response of FRP-confined RC structures.

This research is intended to extend the deterministic seismic design optimization method presented by Zou et al. (2007b) to a reliability-based design approach. A general framework of the reliability-based optimal design is decomposed into three parts: nonlinear structural simulation, reliability analysis, and numerical optimization. To consider the uncertainty of earthquake loading involved in designing a structure, the structural interstory drift response is modeled to be indeterministic, and its probability distribution, mean value, and standard deviation are defined. In this probabilistic approach, the failure probability is defined as the occurrence that an interstory drift response is

larger than its allowable limit. The reliability-based design method is formulated to minimize the FRP cost subject to the prescribed structural reliability constraints. A reliability constraint is considered when the reliability index of the structure response has to fulfill a certain minimum value. Using the results of the non-linear structural analysis and reliability analysis, the interstory drift reliability index constraints are explicitly formulated. A numerical optimality criteria (OC) technique is then developed to solve this reliability-based design optimization problem. To illustrate the effectiveness of the reliability-based design approach, a three-story building example is selected, and numerical results are presented.

FRP-confined concrete

Lam and Teng's model

Studies on FRP-confined concrete have been conducted and various models are available in the literature (De Lorenzis and Tefers, 2003; Lam and Teng, 2003a; Wei and Wu, 2012; Yu et al., 2015). Lam and Teng (2003b) presented a model which is able to capture all major characteristics of the stress-strain relationship of FRP-confined concrete; therefore, it is employed in this study. In this model, the entire stress-strain curve is divided into two segments which are represented using a parabolic function and a linear function, respectively, as

$$\sigma_c = E_c \varepsilon_c - \frac{(E_c - E_2)^2}{4f'_{co}} \varepsilon_c^2 \quad \text{for } 0 \leq \varepsilon_c \leq \varepsilon_t \quad (1a)$$

and

$$\sigma_c = f'_{co} + E_2 \varepsilon_c \quad \text{for } \varepsilon_t \leq \varepsilon_c \leq \varepsilon_{cu} \quad (1b)$$

where

$$E_2 = \frac{f'_{cc} - f'_{co}}{\varepsilon_{cu}} \quad (2)$$

$$\varepsilon_t = \frac{2f'_{co}}{(E_c - E_2)} \quad (3)$$

The following notations are used for FRP-confined concrete: σ_c is the axial stress, ε_c is the axial strain, f'_{cc} is the compressive strength, and ε_{cu} is the ultimate strain, respectively. For unconfined concrete, f'_{co} is the compressive strength and E_c is the tangent elastic modulus, respectively. In equation (1), E_2 is the slope of the straight line segment having an intercept $f_0 = f'_{co}$ on the stress axis; and ε_t is the axial strain corresponding to the point where the parabolic and linear segments meet. Note that

$$\frac{f'_{cc}}{f'_{co}} = 1 + 3.3k_{s1} \frac{f_l}{f'_{co}} \quad (4)$$

$$\frac{\varepsilon_{cu}}{\varepsilon_{co}} = 1.75 + 12k_{s2} \left(\frac{f_l}{f'_{co}} \right) \left(\frac{\varepsilon_{h,rup}}{\varepsilon_{co}} \right)^{0.45} \quad (5)$$

where ε_{co} ($\varepsilon_{co} = 0.002$) is the axial strain at peak stress of unconfined concrete (Lam and Teng, 2003a); $\varepsilon_{h,rup}$ is the hoop rupture strain of the FRP jacket; and f_l is the equivalent confining pressure of FRP. Neglect the confinement provided by the transverse reinforcement; the equivalent confining pressure applied to a rectangular cross section with width B and depth D is given by (Lam and Teng, 2003b)

$$f_l = \frac{2E_{frp}t\varepsilon_{h,rup}}{\sqrt{D^2 + B^2}} \quad (6)$$

E_{frp} is the Young's modulus and t is the thickness of FRP, respectively. It is seen from equation (6) that f_l is linear with respect to t . In equations (4) and (5), two shape factors are introduced to account for the effects of the cross-sectional shape on concrete strength and strain, namely, k_{s1} and k_{s2} , as

$$k_{s1} = \left(\frac{B}{D} \right)^2 \frac{A_e}{A_c} \quad (7)$$

$$k_{s2} = \left(\frac{D}{B} \right)^{0.5} \frac{A_e}{A_c} \quad (8)$$

where A_e and A_c are the effectively confined area of concrete and total FRP-enclosed area of concrete, respectively.

Strength of FRP-confined rectangular cross sections

The FRP-confined concrete model described in the previous section has been applied to the analysis of RC members subjected to combined axial force and bending moment (Teng et al., 2002), and its predictions have been shown to compare favorably with test data (Yuan et al., 2008). For an FRP-confined RC member with a rectangular cross section, the ultimate moment strength M_u and curvature ϕ_u of can be derived and calculated. A number of assumptions are used: the plane cross section remains plane; the steel behavior is assumed to be elastic-perfectly plastic; the lateral confinement is only provided by the FRP jacket; no longitudinal stiffness is provided by the FRP jacket; compression is taken as positive; and the extreme concrete compression fiber reaches the maximum strain in concrete, ε_{cu} , for the strength limit state.

Figure 1 illustrates the stress, strain, and force distribution of a rectangular column section at the

ultimate state, where $f_{s1}, f_{s2}, f_{s3}, \dots$ and $A_{s1}, A_{s2}, A_{s3}, \dots$ are the stresses and the areas of steel, corresponding to the strains, $\varepsilon_{s1}, \varepsilon_{s2}, \varepsilon_{s3}, \dots$, and the steel reinforcement depths, $d_{s1}, d_{s2}, d_{s3}, \dots$, each of which represents the distance from the centroid of steel to the extreme concrete fiber in compression. Two parameters, $\bar{\alpha}$ and $\bar{\gamma}$, are used to characterize the equivalent compressive stress block of concrete (Yuan et al., 2008)

$$\bar{\alpha} = 1 + \frac{E_2 \varepsilon_{cu}}{2f'_{co}} - \frac{2f'_{co}}{3(E_c - E_2)\varepsilon_{cu}} \quad (9)$$

$$\bar{\gamma} = 1 - \frac{-2f'_{co}{}^3 + 3f'_{co}\varepsilon_{cu}^2(E_c - E_2)^2 + 2E_2\varepsilon_{cu}^3(E_c - E_2)^2}{-4f'_{co}{}^2\varepsilon_{cu}(E_c - E_2) + 3E_2\varepsilon_{cu}^3(E_c - E_2)^2 + 6f'_{co}\varepsilon_{cu}^2(E_c - E_2)^2} \quad (10)$$

where $E_2, \varepsilon_{cu}, f'_{cc}$ and further $\bar{\alpha}$ and $\bar{\gamma}$ are found to be functions of the thickness t of the FRP jacket. $E_2, \varepsilon_{cu}, f'_{cc}$ are given by

$$E_2 = \frac{at}{1.75\varepsilon_{co} + bt} \quad (11)$$

$$\varepsilon_{cu} = 1.75\varepsilon_{co} + bt \quad (12)$$

$$f'_{cc} = f'_{co} + at \quad (13)$$

where

$$a = \frac{6.6k_{s1}E_{frp}\varepsilon_{h,rup}}{\sqrt{D^2 + B^2}}; \quad b = \left(\frac{24k_{s2}E_{frp}\varepsilon_{h,rup}\varepsilon_{co}}{f'_{co}\sqrt{D^2 + B^2}} \right) \left(\frac{\varepsilon_{h,rup}}{\varepsilon_{co}} \right)^{0.45} \quad (14)$$

Based on the force equilibrium equation shown in Figure 1, the neutral axis depth X is expressed as

$$X = \frac{P - \sum_{k=1}^{N_{sk}} f_{sk}A_{sk}}{\bar{\alpha}f'_{co}B} \quad (15)$$

where N_s is the total number of rows of steel reinforcement; and A_{sk} and f_{sk} are the cross-sectional area and stress of the k th row of steel reinforcement, respectively. The ultimate moment strength M_u corresponding to P is calculated based on moment equilibrium

$$M_u = \bar{\alpha}f'_{co}BX \left(\frac{D}{2} - \bar{\gamma}X \right) + \sum_{k=1}^{N_s} f_{sk}A_{sk} \left(\frac{D}{2} - d_{si} \right) \quad (16)$$

and the ultimate curvature is determined as

$$\phi_u = \frac{\varepsilon_{cu}}{X} \quad (17)$$

Similarly, the yield curvature, ϕ_y , can be obtained based on the force equilibrium equation at the first yield state (Zou and Chan, 2005).

Reliability-based optimal design problem formulation

Objective function

Retrofitting of columns is a widely used upgrading approach for the rehabilitation of RC moment-resisting frames (Ghobarah et al., 2000). External FRP jackets provide a very effective way of increasing the strength and ductility of RC columns (Teng et al., 2003). As shown in Figure 2, FRP composites are wrapped in the hoop direction as jackets to improve column confinement for enhanced strength and ductility. In this study, FRP cost is defined as the design objective function. Since reliable data for assessing the reliability of FRP cost are not readily available, the design objective function is considered to be deterministic.

For a FRP-retrofitted RC building whose structural system topology is predefined, there are N_{ci} ($i = 1, 2, 3, \dots, N_{ci}$) columns, N_{bi} ($i = N_{ci} + 1, N_{ci} + 2, N_{ci} + 3, \dots, N_{ci} + N_{bi}$) beams, and $2(N_{ci} + N_{bi})$ potential plastic hinges. The plastic hinges are located

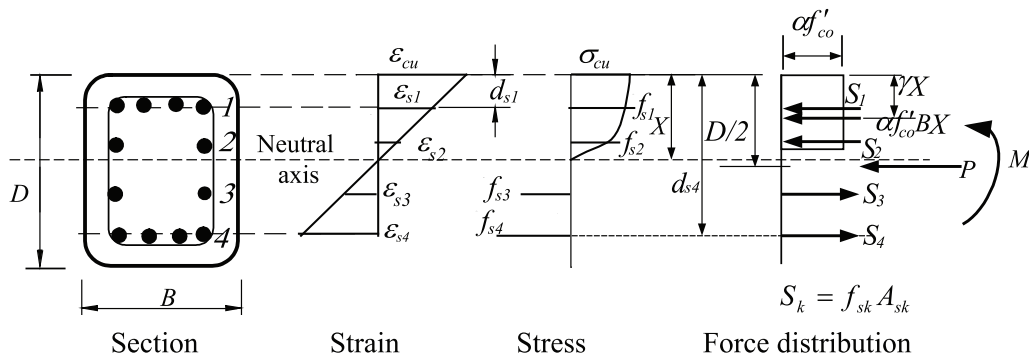


Figure 1. Section with strain, stress, and force distribution.

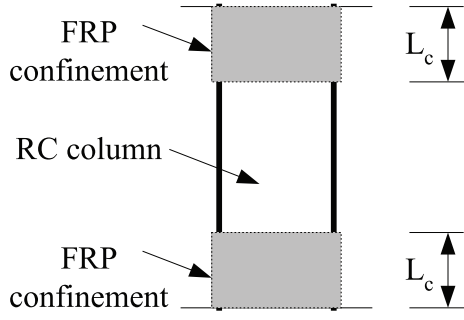


Figure 2. FRP jacket regions for column seismic retrofit (elevation view).

at two ends of structural members, and FRP jackets are used in the plastic hinge regions of columns. The thickness, t_i , of the FRP jacketing is treated as a design variable in optimization. The cost of FRP composite is minimized as

$$\text{Minimize : FRPcost } F(t_i) = \sum_{i=1}^{N_{c_i}} w_i t_i \quad (18)$$

w_i is the cost or weight coefficient of FRP jacket and $w_i = 4L_{c_i}(B_i + D_i)\rho$. Here, it is assumed that each column has a rectangular cross section; ρ is the unit volumetric cost of FRP jacket; and L_{c_i} is the length of the confinement region for the plastic hinge at an end of column i . The length L_{c_i} can be taken as the larger of the plastic hinge length, $0.5d$, and 12.5% of member length (Teng et al., 2002). In this study, only FRP jacket thickness required by moment hinge confinement failure is considered as a design variable, while the jacket thickness required by shear failure and lap splice failure is considered invariant for simplicity. Once the required thickness of FRP is determined, the number of FRP layers can be further determined.

Design variables

Thickness of FRP jacket. For a given type of FRP composite, the FRP thicknesses are selected as deterministic design variables for the study of retrofitting RC buildings, while the structural member dimensions and steel reinforcement areas are fixed. This provides a practical approach that can reduce the size of the design optimization problem to a manageable level (Zou et al., 2007b).

Equivalent static earthquake action and structural responses. It has been well-recognized that the response of structures to earthquakes is a random process with relatively large uncertainties. In the nonlinear

pushover analysis, the equivalent static loads transformed from dynamic earthquake loads are random variables. The structural responses such as the inelastic interstory drift responses and their allowable ratios are also treated as random variables. The external earthquake loading actions usually have relatively larger uncertainties than the uncertainties of structure properties such as the material properties and structural stiffness (Cheng et al., 1998; Li, 2003; Zou et al., 2010). Therefore, the structural stiffness can be approximately taken to be deterministic in optimization formulation. This results in that the statistical properties and probability distributions of the structural responses caused by earthquake actions are the same as those of the external actions.

Structural responses can be local responses such as member strength or global responses including story drifts. It is commonly recognized that among various kinds of structural responses, interstory drift is an important indicator in structural safety under earthquake loading. Furthermore, it is generally acceptable to consider that the probability distributions of the structural responses and earthquake actions are the same, which are usually described by the extreme value distribution Type II (GBJ68-84, 1984; Gao and Bao, 1985; Li and Cheng, 2002). In this research, the interstory drift responses are taken as indeterministic design variables and assumed to have the extreme value Type II distribution.

Assuming an interstory drift ratio $\Delta\bar{u}$ has the extreme value Type II distribution, its cumulative distribution function, denoted by $F_{II}(\Delta\bar{u})$, can be defined as (Gao and Bao, 1985; Zou et al., 2010)

$$F_{II}(\Delta\bar{u}) = \exp\left[-\left(\frac{\alpha}{\Delta\bar{u}}\right)^k\right] \quad (19)$$

and its probability density function $f_{II}(\Delta\bar{u})$ is

$$f_{II}(\Delta\bar{u}) = F'_{II}(\Delta\bar{u}) = \left(\frac{k}{\alpha}\right) \cdot \left(\frac{\alpha}{\Delta\bar{u}}\right)^{k+1} \exp\left[-\left(\frac{\alpha}{\Delta\bar{u}}\right)^k\right] \quad (20)$$

where k is the shape parameter, and α is the largest characteristic value of the initial variable $\Delta\bar{u}$. To calculate the mean value $\mu_{\Delta\bar{u}}$ and standard deviation $\sigma_{\Delta\bar{u}}$ of drift ratio $\Delta\bar{u}$, the following equations are used

$$\mu_{\Delta\bar{u}} = \alpha\Gamma\left(1 - \frac{1}{k}\right) \quad (k > 1) \quad (21)$$

$$\sigma_{\Delta\bar{u}}^2 = \alpha^2 \left[\Gamma\left(1 - \frac{2}{k}\right) - \Gamma^2\left(1 - \frac{1}{k}\right) \right] \quad (k > 2) \quad (22)$$

In equations (21) and (22), Γ denotes a gamma function such that $\Gamma(x) = \int_0^{\infty} e^{-x} x^{x-1} dx$, where x is a variable. Based on equations (21) and (22), the solution of k is determined by

$$\frac{\Gamma(1 - \frac{2}{k})}{\Gamma^2(1 - \frac{1}{k})} - \left(1 + \frac{\sigma_{\Delta\bar{u}}^2}{\mu_{\Delta\bar{u}}^2}\right) = 0 \quad (23)$$

k can be calculated based on equation (23) if the $\sigma_{\Delta\bar{u}}/\mu_{\Delta\bar{u}}$ ratio is known. Substituting k into equation (21) to solve α as

$$\alpha = \frac{\mu_{\Delta\bar{u}}}{\Gamma(1 - \frac{1}{k})} \quad (24)$$

Upon the known values of α and k as well as the standard value $\Delta\bar{u}$ obtained from the pushover analysis, the probabilistic distribution of $\Delta\bar{u}$ can be determined using equations (19) and (20). Since the indeterministic variable $\Delta\bar{u}$ has the extreme value Type II distribution, it is required to first transform it into an equivalent normal distribution (Melchers, 1999). The equivalent normal mean value, $\sigma_{\Delta\bar{u}}^N$, and the equivalent normal standard deviation, $\mu_{\Delta\bar{u}}^N$, can be determined as

$$\sigma_{\Delta\bar{u}}^N = \frac{\phi\{\Phi^{-1}[F_{II}(\Delta\bar{u})]\}}{f_{II}(\Delta\bar{u})} \quad (25)$$

$$\mu_{\Delta\bar{u}}^N = \Delta\bar{u} - \sigma_{\Delta\bar{u}}^N \cdot \Phi^{-1}[F_{II}(\Delta\bar{u})] \quad (26)$$

where $\Phi(\cdot)$ is the standard normal probability distribution function and $\Phi^{-1}(\cdot)$ is the inverse of $\Phi^{-1}(\cdot)$; and $\phi(\cdot)$ represents the standard normal density function.

Allowable interstory drift limits. The allowable story drift limits, denoted by \bar{d} , follow extreme value distribution Type I (Gao and Bao, 1985). The cumulative distribution function $F_I(\bar{d})$ of Type I for \bar{d} can be defined by

$$F_I(\bar{d}) = \exp\left[-\exp\left(-\frac{\bar{d} - k}{\alpha}\right)\right] \quad (27)$$

And the corresponding probability density function can be written as

$$f_I(\bar{d}) = F'_I(\bar{d}) = \frac{1}{\alpha} \exp\left[-\exp\left(-\frac{\bar{d} - k}{\alpha}\right) - \frac{\bar{d} - k}{\alpha}\right] \quad (28)$$

In equations (27) and (28), the parameters, α and k can be determined as follows

$$\alpha = \frac{\sigma_{\bar{d}}}{1.2825} \quad (29)$$

$$k = \mu_{\bar{d}} - 0.5772\alpha \quad (30)$$

In equations (29) and (30), $\mu_{\bar{d}}$ and $\sigma_{\bar{d}}$ are the mean value and its standard deviation of the random variable \bar{d} , respectively. d is defined as a standard value of \bar{d} .

Similarly, once values of α and k obtained from statistical analysis as well as the standard value d obtained from the user or the requirement of design codes, equations (27) and (28) can be used to determine the probabilistic distribution of the random variable \bar{d} . Similar as equations (25) and (26), by transforming \bar{d} into an equivalent normal distribution, the mean value and standard deviation $\sigma_{\bar{d}}^N$ and $\mu_{\bar{d}}^N$ of the equivalent normal distribution are obtained as

$$\sigma_{\bar{d}}^N = \frac{\phi\{\Phi^{-1}[F_I(\bar{d})]\}}{f_I(\bar{d})} \quad (31)$$

$$\mu_{\bar{d}}^N = \bar{d} - \sigma_{\bar{d}}^N \cdot \Phi^{-1}[F_I(\bar{d})] \quad (32)$$

Design constraints

Interstory drift reliability constraints. In reliability-based optimum design of structures subjected to earthquake loads, probabilistic or indeterministic design constraints are typically considered. The indeterministic constraints are classified as member reliability constraints and system reliability constraints, respectively. Structural member reliability is generally considered in design codes as presented earlier. In contrast, there are a large number of possible structural system failure modes. It is commonly known that the interstory drift failure modes are considered as structural system failure modes; and furthermore, the magnitude of interstory drift is an important indicator of damage levels and performance measurement of the structure. Thus, the structural system reliabilities for the performance requirements expressed by the structural story drift reliabilities can be considered as the key indices in the performance-based seismic design (Cheng et al., 1998).

The failure of a structure is defined as the event that the structural response exceeds the acceptable limits measured by the reliability index or failure probability. In the reliability-based optimization, the major design constraint specifies that the structural system must satisfy a minimum level of reliability as represented by specifying the reliability index β_j of the j th interstory drift ratio to be no less than a target value $\bar{\beta}_j$

$$\beta_j \geq \bar{\beta}_j \quad (j = 1, 2, 3, \dots, N_j) \quad (33)$$

N_j is the total number of drift ratio reliability constraints. As the target value $\bar{\beta}_j$ increases, the FRP cost increases and the expected structural failure loss reduces. There is no specific value of $\bar{\beta}_j$ corresponding to interstory drift response in current design codes. A

suitable $\bar{\beta}_j$ should be determined based on a good balance between economic considerations and generally accepted levels of risks (Cheng et al., 1998).

Plastic rotation and sizing bound constraints. Aside from the above-mentioned probabilistic constraints, deterministic design constraints should also be considered. These include construction and FRP jacket thickness requirements. In the optimization iterations, it is necessary to ensure that θ_p is within the specified upper limit of plastic rotation, θ_p^U , for a given performance level. That is to say, the plastic rotation constraints are defined as

$$\theta_{p,i} \leq \theta_p^U \quad (i = 1, 2, 3, \dots, N_{ci}) \quad (34)$$

In addition, the FRP thickness is imposed within the minimum and maximum limits as

$$t_i^L \leq t_i \leq t_i^U \quad (i = 1, 2, 3, \dots, N_{ci}) \quad (35)$$

t_i^U and t_i^L are the upper and lower bounds of variable t_i , respectively.

Reliability analysis

The failure probability P_f can be expressed as

$$P_f = 1 - \Phi(\beta) \quad (36)$$

where β is the reliability index. The computation of the failure probability requires the types of probability distributions (e.g. extreme Type II) and the descriptors (e.g. means, coefficients of variation, and variances) of these random variables. In this work, the first-order second-moment (FOSM) method is used to calculate the reliability index or the failure probability corresponding to a specified interstory drift limit. The FOSM method is an efficient approach to estimate reliability index β then to calculate failure probability P_f . However, it should be noted that the FOSM approach works only with equivalent normal distributions. After transforming non-normally distributed random variables into equivalent normally distributed variables, the reliability index β of the equivalent normal probability distribution is calculated as

$$\beta = \frac{\mu_d^N - \mu_{\Delta\bar{u}}^N}{\sqrt{(\sigma_d^N)^2 + (\sigma_{\Delta\bar{u}}^N)^2}} = \Phi^{-1}(1 - P_f) \quad (37)$$

where $\sigma_{\Delta\bar{u}}^N$ and σ_d^N can be expressed, respectively, by equations (25) and (26) with respect to the random variable $\Delta\bar{u}$; σ_d^N and μ_d^N can be determined, respectively, by equations (31) and (32). As a result, the reliability index β is formulated directly with respect to $\Delta\bar{u}$.

In order to apply gradient-based design optimization methods, $\Delta\bar{u}$ needs to be explicitly expressed with respect to the FRP thickness, t .

Explicit formulation of inelastic displacements

The story drift Δu given in equations (25) and (26) should be expressed using variable t . Details of the formulation were addressed by Zou et al. (2007b), and hence, only a brief presentation is given herein. The virtual work principle is applied to express the push-over displacements using the internal member forces and moments obtained from the nonlinear structural pushover analysis. The story displacement, u_j , includes the virtual work, $u_{j,memb}$, in structural members and the virtual work, $u_{j,hinge}^{beam}$ and $u_{j,hinge}^{col}$, generated by the plastic hinges at beams and columns, respectively. So

$$u_j = (u_{j,memb} + u_{j,hinge}^{beam}) + u_{j,hinge}^{col} \quad (38)$$

in which

$$u_{j,hinge}^{col} = \sum_{i=1}^{N_{ci}} \left[\sum_{h=1}^2 m_{pjh}^0 \theta_{ph} \right]_i \quad (39)$$

In equation (39), m_{pjh}^0 is the virtual end moment at the location of the h th hinge of a member due to a virtual load applied at the location corresponding to the story displacement, u_j ; θ_{ph} is the plastic rotation at the same plastic hinge, and θ_{ph} equals zero if there is no plastic hinge. In the design optimization iterations, $(u_{j,memb} + u_{j,hinge}^{beam})$ is treated as a constant since member dimensions and reinforcement ratios are fixed, and the FRP jackets are only used to confine the columns. The emphasis here is on the displacement, $u_{j,hinge}^{col}$, due to the plastic hinge formation in the FRP-retrofitted columns and changed by the thickness change of the FRP jacket.

In this study, a bilinear curve A–B–C, as shown in Figure 3, is used to model the moment–rotation relationship of a plastic hinge. The plastic rotation, θ_p , is determined as

$$\theta_p = \frac{M - M_y}{M_u - M_y} \theta_p^U \quad (40)$$

where M is the internal moment, M_y is the yield moment, and M_u is the ultimate moment resistance at the plastic hinge, respectively. The yield moment is the bending moment at the first yielding of the tensile steel. In equation (40), θ_p^U is the ultimate plastic rotation, as

$$\theta_p^U = (\phi_u - \phi_y) l_p \quad (41)$$

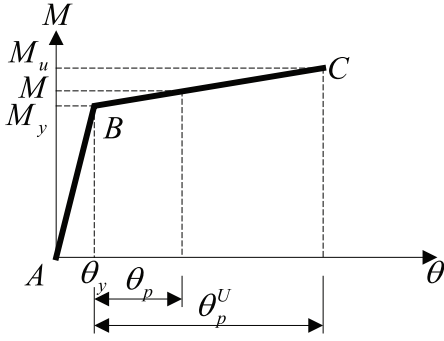


Figure 3. Moment–rotation curve.

In equation (41), ϕ_u and ϕ_y are the ultimate and yield curvatures; l_p is the plastic hinge length. Since the confining pressure capacity provided by the FRP jacket increases with an increase of FRP thickness, the compressive strength and ultimate strain of confined concrete (i.e. f_{cc}^t and ε_{cu}) are significantly improved resulting in an increase in M_u and θ_p^U , while the FRP jacket has no effect on the value of M_y . The details of the formulation of M_y , independent of t , were introduced by Zou and Chan (2005).

It is found from equations (15) to (17) that X , M_u , and ϕ_y can be expressed in terms of t due to the fact that ε_{cu} , $\bar{\alpha}$, and $\bar{\gamma}$ are all functions of t . As a result, θ_p in equation (40) can be expressed in terms of t . In order to simplify the highly nonlinear formulation of θ_p in the optimum design process, a second-order Taylor series expansion of θ_p at an initial point t^0 is written as (Zou et al., 2007b)

$$\theta_p(t) = \theta_p|_{t=t^0} + \frac{\partial\theta_p}{\partial t}|_{t=t^0}(t-t^0) + \frac{1}{2}\frac{\partial^2\theta_p}{\partial t^2}|_{t=t^0}(t-t^0)^2 \quad (42)$$

where the gradient, $\partial\theta_p/\partial t$, and the second-order derivative, $\partial^2\theta_p/\partial t^2$, can be analytically derived based on equation (40). If the explicit plastic rotation $\theta_p(t)$ is substituted into equations (38) and (39), the interstory drift, Δu_j , at the j th story level can also be expressed with respect to the design variable, t_i , as

$$\begin{aligned} \Delta u_j(t_i) &= \Delta u_j|_{t_i=t_i^0} \\ &+ \sum_{i=1}^{N_{ci}} \frac{\partial\Delta u_j}{\partial t_i}|_{t_i=t_i^0}(t_i-t_i^0) + \frac{1}{2}\sum_{i=1}^{N_{ci}} \frac{\partial^2\Delta u_j}{\partial t_i^2}|_{t_i=t_i^0}(t_i-t_i^0)^2 \end{aligned} \quad (43)$$

Explicit formulation of design constraints on reliability index given in equation (33) can be derived based on equation (43). Finally, the reliability-based inelastic structural design problem is formulated with respect to

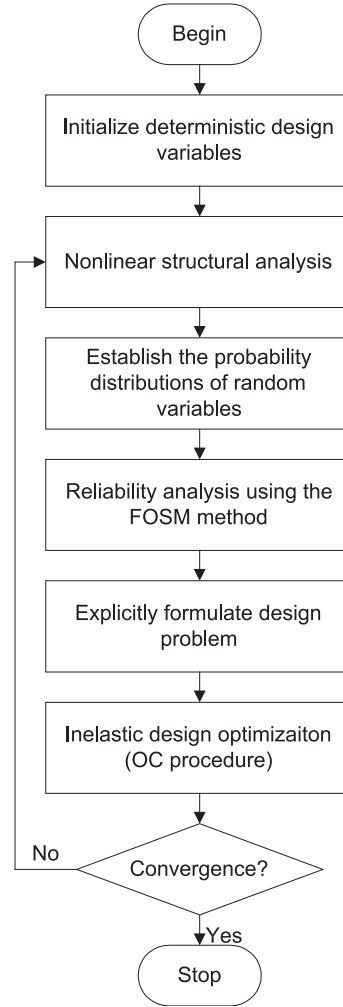


Figure 4. Flowchart of reliability-based structural design optimization.

the deterministic variable, t . The OC method can then be iteratively applied to find an optimal design.

Reliability-based design procedure

The procedure of reliability-based structural optimization is outlined as follows, and the flow chart for the procedure can be found in Figure 4:

1. Assume initial value of the FRP thickness for each column and estimate its upper and lower bounds. Choose the appropriate target reliability index $\bar{\beta}_j$ of interstory drifts. For each random variable, determine the coefficient of variation and the ratio of mean value over standard value;
2. Conduct nonlinear pushover structural analysis and determine the standard values of random variables;

3. Establish probability distributions of all random variables. $F_{II}(\Delta\bar{u})$ and $f_{II}(\Delta\bar{u})$ are established for $\Delta\bar{u}$ based on equations (19) and (20). Also, $F_I(\bar{d})$ and $f_I(\bar{d})$ are determined for the random variable \bar{d} using equations (27) and (28);
4. Use the FOSM method to perform the reliability analysis. The actual probability distributions are converted into equivalent normal distributions using equations (25) and (26) and equations (31) and (32);
5. Explicitly formulate the reliability-based optimization problem, using equation (18) and equations (33) to (35);
6. Carry out the design optimization using the iterative OC method;
7. Perform the convergence check. If the change in objective value and the constraint violations are satisfied, stop the design; otherwise, go back to Step 2 to start the next optimization cycle.

An illustrative example

A three-story, three-bay RC framework shown in Figure 5 is employed to study the proposed reliability-based inelastic design method. The material properties are selected as follows: the unconfined compressive strength of concrete is 21 MPa, and the yield strength of steel reinforcement is 300 MPa. All beams are 250×600 mm with the top and bottom reinforcement ratios of 1.1% and 0.9%, respectively. The exterior columns (C1, C3, and C5) are $300 \text{ mm} \times 300$ mm with a reinforcement ratio of 1.25% and the interior columns (C2, C4, and C6) are $400 \text{ mm} \times 400$ mm with a reinforcement ratio of 1%. The shear resistance of the existing retrofitted frames was determined to be greater than the shear demand based on the Chinese design code (GBJ68-84). The behavior of the RC building is governed by the flexural failure of frame members.

The nonlinear structural pushover analysis is performed using the SAP2000 software package (Computer and Structures, Inc. (CSI), 2000) for

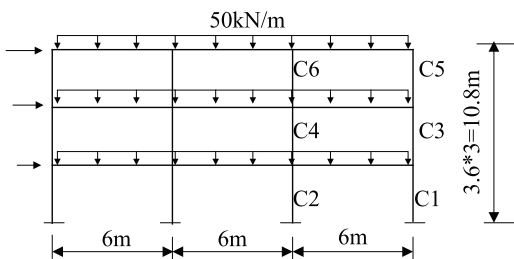


Figure 5. A three-story three-bay RC retrofitted frame.

examining the retrofit effect and estimating the performance of the original as well as the retrofitted structures. The pushover analysis incorporates vertical gravity loads and lateral seismic loads as shown in Figure 5. In the pushover analysis, the gravity loads are remained unchanged, while the lateral loads are incrementally updated and applied on the structure. The initial lateral loads applied on the structure are proportional to the product of the first mode shape of the structure and the story mass. The beams and columns are modeled as line elements with plastic hinges at both ends of the members. The plastic hinges at both ends of all beams are flexural moment hinges, and their ultimate rotation θ_p^U is taken as 0.02 rad (ATC, 1996). The plastic hinges at both ends of all columns are axial-moment hinges. The ultimate rotation θ_p^U of these hinges is not a constant in the design optimization process; its value varies with the thickness of the FRP jacket.

The FRP composites are used to retrofit all the columns in the RC building. The elastic modulus E_{frp} and tensile strength f_{frp} of FRP are 230,000 and 3550 MPa, respectively. At a hoop rupture strain of $\varepsilon_{h,rupt} = 0.00913$, the tensile stress of FRP is 2100 MPa. The distance R_c from the surface of the concrete to the center of the reinforcements is assumed to be 50 mm. The lower limit of the FRP thicknesses is assumed to be the 0.0, and there is no upper limit used. The lower limit value is taken as the starting point for each column in the inelastic design optimization. The objective function is to minimize the FRP volume subject to the reliability index constraints corresponding to inelastic interstory drift responses. A ratio of 1% is used as the allowable inelastic interstory drift limit. The convergence criteria are met when the objectives for two consecutive design cycles are less than 0.5% and the difference between the displacement and the limiting value for an active drift constraint is within 0.5%.

Based on the research results by Gao and Bao (1985), Li and Cheng (2002), and Zou et al. (2010), during a 50-year return period, it is found from statistical study that the relationship between the mean value $\mu_{\Delta\bar{u}}$ and standard value Δu is $\mu_{\Delta\bar{u}} = 0.597\Delta u$; the coefficient of variation $\delta_{\Delta\bar{u}}$ (i.e. the ratio of standard deviation $\sigma_{\Delta\bar{u}}$ over mean value $\mu_{\Delta\bar{u}}$) is 1.267, that is, the relationship between the standard deviation $\sigma_{\Delta\bar{u}}$ and mean value $\mu_{\Delta\bar{u}}$ is $\sigma_{\Delta\bar{u}} = 1.267\mu_{\Delta\bar{u}}$. Thereby, $\sigma_{\Delta\bar{u}}$ is derived as

$$\sigma_{\Delta\bar{u}} = 1.267 \times 0.597\Delta u = 0.756\Delta u$$

Substituting $\delta_{\Delta\bar{u}} = 1.267$ into equation (23), k can be calculated as 2.35. Substituting this and $\mu_{\Delta\bar{u}} = 0.597\Delta u$ into equation (24) and solve for parameter α

$$\alpha = \frac{0.597\Delta u}{\Gamma\left(1 - \frac{1}{2.35}\right)} = 0.385\Delta u$$

Therefore, $F_{II}(\Delta\bar{u})$ and $f_{II}(\Delta\bar{u})$ given in equations (19) and (20) can be expressed with respect to the random variable $\Delta\bar{u}$ as

$$F_{II}(\Delta\bar{u}) = \exp\left[-\left(\frac{0.385\Delta u}{\Delta\bar{u}}\right)^{2.35}\right]$$

$$f_{II}(\Delta\bar{u}) = F'_{II}(\Delta\bar{u}) = \left(\frac{0.249}{\Delta\bar{u}^{3.35}} \cdot \frac{1}{\Delta u}\right) \exp\left[-\left(\frac{0.385\Delta u}{\Delta\bar{u}}\right)^{2.35}\right]$$

Once the standard value Δu is obtained from the pushover analysis, the probabilistic distribution of $\Delta\bar{u}$ can be determined and further transformed into an equivalent normal distribution using equations (25) and (26), namely, $\sigma_{\Delta\bar{u}}^N$ and $\mu_{\Delta\bar{u}}^N$, which are written with respect to $\Delta\bar{u}$ as

$$\sigma_{\Delta\bar{u}}^N = \frac{\phi\left\{\Phi^{-1}\left[e^{-\left(\frac{0.385\Delta u}{\Delta\bar{u}}\right)^{2.35}}\right]\right\}}{\left(\frac{0.249}{\Delta\bar{u}^{3.35}} \cdot \frac{1}{\Delta u}\right) \exp\left[-\left(\frac{0.385\Delta u}{\Delta\bar{u}}\right)^{2.35}\right]}$$

$$\mu_{\Delta\bar{u}}^N = \Delta\bar{u} - \frac{\phi\left\{\Phi^{-1}\left[e^{-\left(\frac{0.385\Delta u}{\Delta\bar{u}}\right)^{2.35}}\right]\right\}}{\left(\frac{0.249}{\Delta\bar{u}^{3.35}} \cdot \frac{1}{\Delta u}\right) \exp\left[-\left(\frac{0.385\Delta u}{\Delta\bar{u}}\right)^{2.35}\right]} \cdot \Phi^{-1}\left[e^{-\left(\frac{0.385\Delta u}{\Delta\bar{u}}\right)^{2.35}}\right]$$

In addition, based on the research results of Gao and Bao (1985), during a 50-year return period, the relationship between the mean value $\mu_{\bar{d}}$ and standard value d is $\mu_{\bar{d}} = 1.02d$; the coefficient of variation is 0.399, that is, the relationship between the standard deviation $\sigma_{\bar{d}}$ and mean value $\mu_{\bar{d}}$ is $\sigma_{\bar{d}} = 0.399\mu_{\bar{d}}$. Therefore

$$\sigma_{\bar{d}} = \delta_{\bar{d}}\mu_{\bar{d}} = 0.399 \times 1.02d = 0.407d$$

The parameters α and k in equations (29) and (30) are rewritten as

$$\alpha = \frac{0.407d}{1.2825} = 0.3173d$$

$$k = 1.02d - 0.5772 \times 0.3173d = 0.837d$$

As a result, $F_I(\bar{d})$ and $f_I(\bar{d})$ in equations (27) and (28) are rewritten as

$$F_I(\bar{d}) = \exp\left[-\exp\left(-\frac{\bar{d} - 0.837d}{0.317d}\right)\right]$$

$$f_I(\bar{d}) = \frac{1}{0.317d} \exp\left[-\exp\left(-\frac{\bar{d} - 0.837d}{0.317d}\right) - \frac{\bar{d} - 0.837d}{0.317d}\right]$$

Similarly, equivalent normal mean value and standard deviation, $\sigma_{\bar{d}}^N$ and $\mu_{\bar{d}}^N$, are obtained based on equations (31) and (32). Upon formulating $\sigma_{\Delta\bar{u}}^N$, $\mu_{\Delta\bar{u}}^N$,

$\sigma_{\bar{d}}^N$, and $\mu_{\bar{d}}^N$, reliability analysis is conducted using the FOSM method. Then, the corresponding mean value, standard deviation, the value of the random variable $\Delta\bar{u}$ can be obtained. Eventually, the reliability index β has an explicit expression with respect to the interstory drift ratio and furthermore with respect to the design variable, the thickness of the FRP. The target index is assumed to be 1.2 corresponding to the failure probability of 11% in this example.

Three cases are selected to commence the reliability-based optimal design in order to study the effect of different initial thicknesses on the convergence of the final design. These are defined as

1. *Case 1.* A deterministic design—deterministic inelastic interstory drift constraints are considered. The initial design values are the lower bound thickness of 0.0 mm;
2. *Case 2.* A reliability-based design—in the optimization formulation, interstory drift reliability index constraints are considered. The optimal FRP thicknesses found by the deterministic design in Case 1 are taken as the initial values.
3. *Case 3.* A reliability-based design—in the optimization formulation, interstory drift reliability index constraints are considered. The lower bound thickness of 0.0 mm is taken as the initial starting point.

Figure 6 plots the convergence histories of the three cases. The design convergence of the deterministic and probabilistic optimal designs is found to be smooth and steady. It is also found that although the starting points in Case 2 and Case 3 are different, the final optimal design objectives are almost the same, that is, $3.402 \times 10^{-2} \text{ m}^3$ for Case 2 and $3.410 \times 10^{-2} \text{ m}^3$ for Case 3. It indicates that the reliability-based optimal structure design is slightly dependent on initial values, as the case of the deterministic optimal design. Besides, the FRP volumes of Cases 2 and 3 are found to be higher than that of $2.046 \times 10^{-2} \text{ m}^3$ in Case 1. The main reason lies in that the target reliability index of 1.20 specified in Cases 2 and 3 is indeed higher than 1.0 that is found from the deterministic drift design (i.e. Case 1), resulting in a higher FRP volume.

Table 1 lists initial and final FRP thicknesses in the three design cases. The FRP values in Cases 2 and 3 are found to be larger than those in Case 1. It is also seen that Cases 2 and 3 result in similar optimal FRP thicknesses although their initial FRP values are quite different. It further indicates that in reliability-based design optimization, the optimal FRP distribution is also independent of the initial values. Table 2 presents the standard value Δu , normalized mean value $\mu_{\Delta\bar{u}}^N$, and normalized standard deviations $\sigma_{\Delta\bar{u}}^N$ of $\Delta\bar{u}$ before

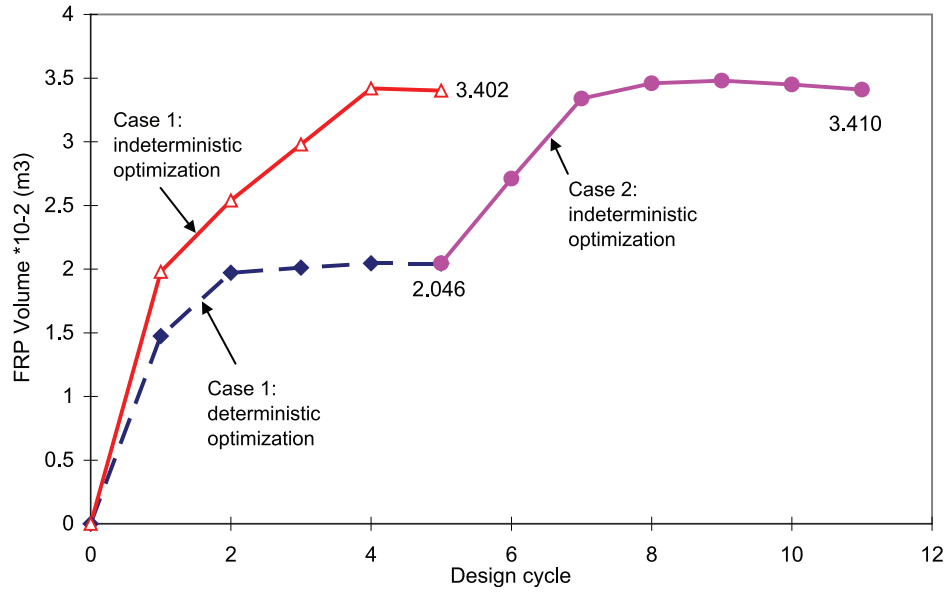


Figure 6. Design histories.

Table 1. Initial and optimal thickness of FRP jacket.

Element type	Story level	Member group	Case 1		Case 2		Case 3	
			Initial t_{frp} (mm)	Optimal t_{frp} (mm)	Initial t_{frp} (mm)	Optimal t_{frp} (mm)	Initial t_{frp} (mm)	Optimal t_{frp} (mm)
Columns	Third	C5	0.000	0.000	0.000	0.000	0.000	0.000
		C6	0.000	0.000	0.000	0.000	0.000	0.000
	Second	C3	0.000	0.282	0.282	0.968	0.000	0.947
		C4	0.000	0.956	0.956	1.943	0.000	1.997
	First	C1	0.000	0.773	0.773	0.919	0.000	0.979
		C2	0.000	1.792	1.792	2.553	0.000	2.376

FRP: fiber-reinforced polymer.

Table 2. Normalized mean values and standard deviations of variable $\Delta\bar{u}$.

Cases	Story level	Initial state			Final state		
		Δu (m)	$\mu_{\Delta\bar{u}}^N$ (m)	$\sigma_{\Delta\bar{u}}^N$ (m)	Δu (m)	$\mu_{\Delta\bar{u}}^N$ (m)	$\sigma_{\Delta\bar{u}}^N$ (m)
Case 2	3	0.01623	-0.01704	0.02365	0.01842	-0.01280	0.02304
	2	0.03607	0.00998	0.01928	0.03204	0.00608	0.01991
	1	0.03599	0.00991	0.01930	0.03260	0.00665	0.01982
Case 3	3	0.01365	-0.02246	0.02427	0.01844	-0.01277	0.02303
	2	0.03646	0.01033	0.01923	0.03190	0.00572	0.01997
	1	0.04726	0.01870	0.01805	0.03206	0.00610	0.01991

and after design optimization. After optimization, Δu , $\mu_{\Delta\bar{u}}^N$, and $\sigma_{\Delta\bar{u}}^N$ in Case 2 are similar as those in Case 3, although their initial values are rather different.

Figure 7 presents the comparisons of the initial and final reliability indices among the three cases. The

reliability index constraints of the first and second stories are initially violated in Cases 2 and 3. In particular, the initial first-story drift reliability index is found to be 0.7 which corresponds to the failure probability of 44% as shown in Figure 7. The results of the

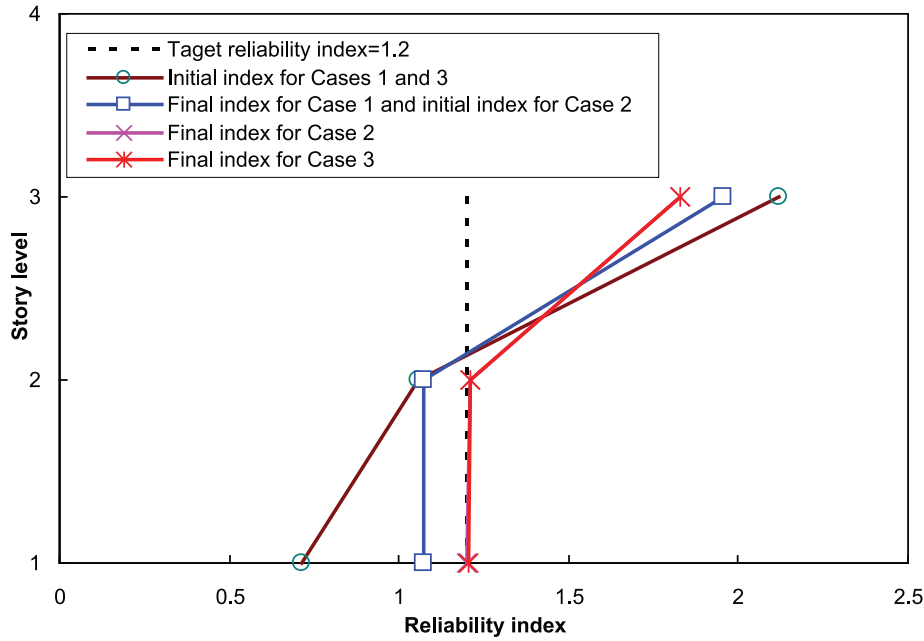


Figure 7. Initial and final reliability indices.

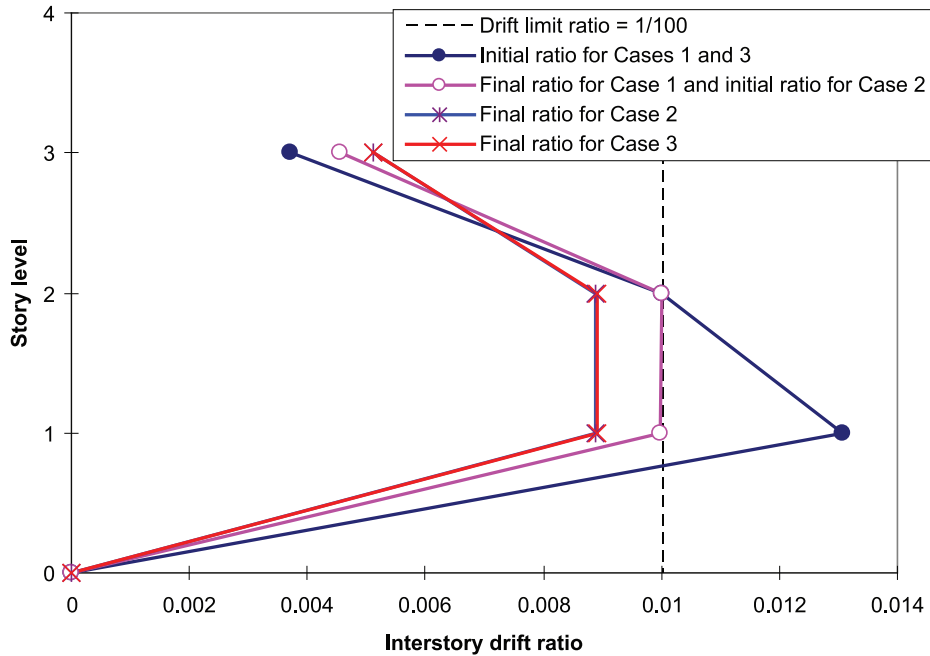


Figure 8. Inelastic interstory drift ratios.

reliability-based designs in Cases 2 and 3 show that all the reliability indices are close to $\beta_j = 1.2$. Such a result indicates that in the reliability-based inelastic structural optimal design, the lateral load resisting system can still be improved by the optimization algorithm to distribute the FRP thickness of all columns so

that lateral inelastic drifts are reduced and the reliability index constraints are satisfied. Moreover, it is found that in Case 1, the final indices of the first- and second-story levels are about 1.0 (corresponding to a failure probability of 16%), which is less than $\beta_j = 1.2$ (corresponding to the failure probability of 11%). It is

clearly demonstrated that deterministic design optimization results do not guarantee a satisfactory reliability index.

The inelastic interstory drift responses of initial and final designs are shown in Figure 8. The final first- and second-story drift ratios in Cases 2 and 3 are very similar but far less than the limit of 1%, while those in Case 1 are close to the drift ratio limit of 1%. There are smaller interstory drift values in the first- and second-story levels in Cases 2 and 3. The reliability-based designs result in stiffer structures with smaller values of interstory drifts, due to the higher levels of reliability imposed.

Conclusion

The reliability-based optimization problem for FRP-retrofitted buildings has been formulated such that not only it can minimize the FRP cost but also satisfy the required reliability constraints due to the uncertainties of seismic loadings. The proposed reliability-based optimization technique integrates inelastic structural analysis using the pushover analysis method, reliability analysis using the FOSM method, and an optimization technique using the OC method. Although these are three independent procedures, reliability-based optimization requires repeated applications of these three procedures until the solution convergence is achieved.

The proposed algorithm converges smoothly and steadily, and is weakly dependent on the initial sizes selected to commence the design iterations; it is able to optimize a reliability-based FRP-retrofitted RC buildings and to distribute its lateral stiffness to satisfy interstory drift reliability index constraints with a minimum FRP cost. In addition, the reliability-based design is able to ensure optimal reliability designs of building structures through the consideration of design constraints that fulfill a target value of the required reliability index for each story, which cannot be achieved in a deterministic optimal design. The proposed design optimization method provides a foundation for future development; other types of uncertainties such as structural modeling uncertainties can be further considered and incorporated.

Declaration of Conflicting Interests

The author(s) declared no potential conflicts of interest with respect to the research, authorship, and/or publication of this article.

Funding

The author(s) disclosed receipt of the following financial support for the research, authorship, and/or publication of this article: The work described in this paper was supported by

grants from the National Natural Science Foundation of China (project no. 51378134, 51578169).

References

- Ang AH and Cornell CA (1974) Reliability bases of structural safety and design. *Journal of Structural Engineering: ASCE* 100(ST9): 1755–1769.
- Applied Technology Council (ATC) (1996) *Seismic evaluation and retrofit of concrete buildings—volume 1 (ATC-40)*. Report no. SSC 96-01. Redwood City, CA: ATC.
- Beck JL, Papadimitriou C, Chan E, et al. (1998) *A performance-based optimal structural design methodology*. Report no. EERL 97-30. Pasadena, CA: Earthquake Engineering Research Laboratory, California Institute of Technology.
- Bertero RD and Bertero VV (2002) Performance-based seismic engineering: the need for a reliable conceptual comprehensive approach. *Earthquake Engineering & Structural Dynamics* 31: 627–652.
- Cao VV and Ronagh HR (2014) Reducing the seismic damage of reinforced concrete frames using FRP confinement. *Composite Structures* 118: 403–415.
- Chan CM and Zou XK (2004) Elastic and inelastic drift performance optimization for reinforced concrete building under earthquake loads. *Earthquake Engineering & Structural Dynamics* 33(8): 929–950.
- Chang CC, Ger JF and Cheng FY (1994) Reliability-based optimum design for UBC and nondeterministic seismic spectra. *Journal of Structural Engineering: ASCE* 120(1): 139–160.
- Charney FA (2000) Needs in the development of a comprehensive performance based design optimization process. In: *Advanced technology in structural engineering: structural congress 2000*, Philadelphia, PA (ed M Elgaaly), 8–10 May (CD-ROM). Reston, VA: ASCE.
- Cheng GD, Li G and Cai Y (1998) Reliability-based structural optimization under hazard loads. *Structural Optimization* 16: 128–135.
- Choi SW (2017) Investigation on the seismic retrofit positions of FRP jackets for RC frames using multi-objective optimization. *Composites Part B: Engineering* 123: 34–44.
- Choi SW, Kim Y and Park HS (2014) Multi-objective seismic retrofit method for using FRP jackets in shear-critical reinforced concrete frames. *Composites Part B: Engineering* 56: 207–216.
- Computer and Structures, Inc. (CSI) (2000) *SAP2000/NL-PUSH Software, Version 7.40*. Berkeley, CA: CSI.
- De Lorenzis L and Tepfers R (2003) A comparative study of models on confinement of concrete cylinders with FRP composites. *Journal of Composites for Construction: ASCE* 7(3): 219–237.
- Federal Emergency Management Agency (FEMA) (2006) *Next-Generation performance-based seismic design guidelines, program plan for new and existing buildings*. Developed by the Applied Research Council for the Federal Emergency Management Agency, Report no. FEMA 445. Washington, DC.
- Foley CM (2002) Optimized performance-based design for buildings. In: SA Burns (ed.) *Recent Advances in Optimal*

- Structural Design*. Reston, VA: American Society of Civil Engineers, pp. 169–240.
- Fragiadakis M, Lagaros ND and Papadrakakis M (2006) Performance-based multiobjective optimum design of steel structures considering life-cycle cost. *Structural and Multidisciplinary Optimization* 32(1): 1–11.
- Frangopol DM (1985) Structural optimization using reliability concepts design. *Journal of Structural Engineering: ASCE* 111(11): 2288–2301.
- Frangopol DM (1997) How to incorporate reliability in structural optimization. In: JS Arora (ed.) *Guide to Structural Optimization (ASCE manuals and reports on engineering practice no. 90)*. Reston, VA: American Society of Civil Engineers, pp. 211–235.
- Frangopol DM and Klisinski M (1989) Material behavior and optimum design of structural systems. *Journal of Structural Engineering: ASCE* 115(5): 1054–1075.
- Frangopol DM and Moses F (1994) Reliability-based structural optimization. In: Adeli H (ed.) *Advances in Design Optimization*. London: Chapman & Hall, pp. 492–570.
- Gao XW and Bao AB (1985) Probabilistic model and its statistical parameters for seismic load. *Earthquake Engineering and Engineering Vibration* 5(1): 13–22.
- Gaxiola-Camacho JR, Azizoltani H, Villegas-Mercado FJ, et al. (2017) A novel reliability technique for implementation of performance-based seismic design of structures. *Engineering Structures* 142: 137–147.
- GBJ68-84 (1984) Uniform standards for design of building structures.
- Ghobarah A, El-Attar M and Aly NM (2000) Evaluation of retrofit strategies for reinforced concrete columns: a case study. *Engineering Structures* 22(5): 490–501.
- Kim SH and Wen YK (1990) Optimization of structures under stochastic loads. *Structural Safety* 7(2–4): 177–190.
- Lagaros ND, Garavelas AT and Papadrakakis M (2008) Innovative seismic design optimization with reliability constraints. *Computer Methods in Applied Mechanics and Engineering* 198(1): 28–41.
- Lam L and Teng JG (2003a) Design-oriented stress-strain model for FRP-confined concrete. *Construction and Building Materials* 17: 471–489.
- Lam L and Teng JG (2003b) Design-oriented stress-strain model for FRP-confined concrete in rectangular columns. *Journal of Reinforced Plastics and Composites* 22(13): 1149–1184.
- Li G (2003) Statistical properties of the maximum elastoplastic story drift of steel frames. *Earthquake Load, Steel & Composite Structures an International Journal* 3(3): 185–198.
- Li G and Cheng GD (2002) Probability distribution of story drift of seismic RC frames. *Journal of Dalian University of Technology* 42(3): 153–157.
- Melchers RE (1999) *Structural Reliability, Analysis and Prediction*. 2nd ed. Chichester: John Wiley & Sons.
- Moses F (1969) Approach to structural reliability and optimization. In: Cohn MZ (ed.) *An Introduction to Structural Optimization* (Study no. 1). Waterloo, ON, Canada: Solid Mechanics Division, University of Waterloo, pp. 81–120.
- Shin J, Scott DW, Stewart LK, et al. (2016) Dynamic response of a full-scale reinforced concrete building frame retrofitted with FRP column jackets. *Engineering Structures* 125: 244–253.
- Song JL and Ellingwood BR (1999) Seismic reliability of space moment steel frames with welded connections: I and II. *Journal of Structural Engineering: ASCE* 125(4): 357–384.
- Teng JG and Lam L (2004) Behavior and modeling of fiber reinforced polymer-confined concrete. *Journal of Structural Engineering: ASCE* 130(11): 1713–1723.
- Teng JG, Chen JF, Smith ST, et al. (2002) *FRP-Strengthened RC Structures*. New York: Wiley.
- Teng JG, Chen JF, Smith ST, et al. (2003) Behavior and strength of FRP-strengthened RC structures: a state-of-the-art review. *Proceedings of the Institution of Civil Engineers: Structures and Buildings* 156(1): 51–62.
- Wei Y-Y and Wu Y-F (2012) Unified stress-strain model of concrete for FRP-confined columns. *Construction and Building Materials* 26: 381–392.
- Wen YK (1995) Building reliability and code reliability. *Earthquake Spectra* 11(2): 269–296.
- Wen YK (2001) Reliability and performance based design. *Structural Safety* 23: 407–428.
- Yu T, Zhang B and Teng GJ (2015) Unified cyclic stress-strain model for normal and high strength concrete confined with FRP. *Engineering Structures* 102: 189–201.
- Yuan F and Wu Y-F (2017) Effect of load cycling on plastic hinge length in RC columns. *Engineering Structures* 147: 90–102.
- Yuan XF, Xia SH, Lam L, et al. (2008) Analysis and behavior of FRP-confined short concrete columns subjected to eccentric loading. *Journal of Zhejiang University: Science A* 9(1): 38–49.
- Zameeruddin M and Sangle KK (2016) Review on recent developments in the performance-based seismic design of reinforced concrete structures. *Structures* 6: 119–133.
- Zou XK and Chan CM (2005) Optimal seismic performance-based design of reinforced concrete buildings using nonlinear pushover analysis. *Engineering Structures* 27: 1289–1302.
- Zou XK, Chan CM, Li G, et al. (2007a) Multiobjective optimization for performance-based design of concrete structures. *Journal of Structural Engineering: ASCE* 133(10): 1462–1474.
- Zou XK, Teng JG, Lorenzis LD, et al. (2007b) Optimal performance-based seismic retrofit design of RC frames using FRP confinement. *Composites Part B: Engineering* 38: 584–597.
- Zou XK, Wang Q, Li G, et al. (2010) Integrated reliability-based seismic drift design optimization of base-isolated concrete buildings. *Journal of Structural Engineering: ASCE* 136(10): 1282–1295.
- Zou XK. (2012) Optimal Seismic Performance-Based Design of Reinforced Concrete Buildings. *Structural Seismic Design Optimization and Earthquake Engineering: Formulations and Applications*, IGI Global, Chapter 9: 208–231.
- Zou XK, Lee HY, Chan E, Xiang P. (2014) Cost Design Optimization of Concrete Transfer Beam Structures. *HKIE Transactions*, The Hong Kong Institution of Engineers, 21(3): 178–191.